A Surface Integral Equations Method for Homogeneous Optical Fibers and Coupled Image Lines of Arbitrary Cross Sections

CHING-CHUAN SU

Abstract—**Based on the surface integral equations, a novel method is developed to treat the propagation characteristics of homogeneous optical fibers of arbitrary cross sections in both the rigorous vectorial and the approximate scalar formulations. This method is ready to be generalized to the cases of multiple dielectric waveguides, such as the coupled dielectric image lines used in microwave integrated circuits. Further, Green's function at cutoff is presented so that the corresponding cutoff frequencies can be treated. Numerical results of propagation characteristics of single and double waveguides are presented in both the vector and scalar forms.**

I. Introduction

IN THE TREATMENT OF propagation characteristics of homogeneous optical fibers with arbitrary cross sections, several numerical methods have been proposed. Among them, Goell [1] has developed the method of circular-harmonic expansion, in which the interior and the exterior fields are expanded respectively in the Bessel and the modified Bessel functions with unknown coefficients. The propagation constants of guided modes, as well as such coefficients, are determined by solving a matrix equation which, in turn, results from matching the four kinds of tangential fields around the boundary of the core region. This expansion method is rigorous in formulation; however, numerical trouble occurs if the cross section becomes rather elongated [1]–[3]. Using the extended boundary condition, Eyges *et al.* [4] and Morita [5] have proposed the scalar form via a transverse field and the vector form via the longitudinal fields [4] or two transverse electric fields [5]. In such methods of extended boundary condition, the interior fields are also expanded in the Bessel functions with unknown coefficients which can be solved by further relating them through some surface integrals pertaining to the exterior region. Other methods capable of treating arbitrarily-shaped fibers include the generalized telegraphist's equation [6], the method of effective cross section [7], and the variational formula [8], which incorporate some approximation in their formulations and will not be discussed further.

Manuscript received February 4, 1985; revised May 20, 1985.

The author was with the Department of Electrical Engineering, National Taiwan University, Taipei, Taiwan, Republic of China. He is now with the Department of Electrical Engineering, National Tsing Hua University, Hsinchu, Taiwan, R.O.C.

As for the more complicated structure of multiple waveguides embedded in a homogeneous medium, Marcatili [9] has presented the transcendental equations for rectangular waveguides, from which propagation constants of guided modes can be found in closed form. These equations are obtained by neglecting the boundary conditions in some regions where the field intensity is usually small and, consequently, simplifying the two-dimensional propagation problem into that of slab waveguides. Besides, Solbach and Wolff [10] have proposed a rigorous method in which the exterior and the interior fields are expanded in plane waves (standing or evanescent) after the introduction of an artificial shielding plate. The calculated results are reported to agree with the experimental data for single and coupled dielectric image lines of rectangular cross sections.

In this investigation, based on the surface integral equations, a novel method is proposed to treat the propagation characteristics of homogeneous dielectric waveguides of arbitrary cross sections in both the rigorous vector and the scalar forms. This method is ready to be generalized to the cases of multiple waveguides embedded in a single surrounding medium, which include the coupled dielectric image lines used in microwave integrated circuits. Further, Green's function (for the cladding region) at cutoff is presented so that the proposed method is capable of treating cutoff frequencies of the aforementioned guiding structures.

The surface integral equations are formulated in Section II to relate the associated fields and their normal derivatives at the boundaries of dielectric cylinders. In Section III, the Green's function at cutoff is presented. Then the propagation characteristics of guided modes can be determined by point-matching at such boundaries the normal derivatives for the scalar form or the four kinds of tangential fields (deduced from the associated fields and their normal derivatives) for the rigorous vector form. Numerical results of single and double waveguides with circular and rectangular cross sections are presented in Section V for both the vector and scalar forms.

II. Formulation

Consider a guiding structure composed of several homogeneous dielectric cylinders with arbitrary cross sections

0018-9480/85/1100-1114$01.00 ©1985 IEEE

embedded in a single surrounding medium as depicted in Fig. 1(a); along such a structure, a time-harmonic electromagnetic wave of angular frequency ω propagates with a propagation constant β in the axial (z) direction. Since the dielectric materials encountered in such a structure are regionally homogeneous, the fields satisfy the scalar Helmholtz equation in each region as stated by

$$\nabla_t^2 F(\bar{r}) + k^2 F(\bar{r}) = 0 \tag{1}$$

where F denotes any field component in rectangular coordinates, ∇_t^2 denotes the Laplacian operator in a transverse plane, $k^2 = k_0^2\epsilon - \beta^2$ (the subscript of ϵ, as well as those of $\hat{l}$ and $\hat{n}$ (Fig. 1(a)) in later discussions, is ignored), and k_0 is the free-space propagation constant. Using Green's second identity, the differential equation (1) for a homogeneous region R can be converted to an integral equation as

$$\int_R \left[F(\bar{r}')\nabla_t^2 G(k,\bar{r},\bar{r}') - G(k,\bar{r},\bar{r}')\nabla_t^2 F(\bar{r}')\right] d\bar{r}'$$
$$= \oint_C \left[-F(\bar{r}')\frac{dG(k,\bar{r},\bar{r}')}{dn} + G(k,\bar{r},\bar{r}')\frac{dF(\bar{r}')}{dn}\right] d\bar{r}' \tag{2}$$

where the left-hand side is a volume integral over the transverse-plane region R, the right-hand side is a closed surface integral over the boundary contour C (the surface of R), and d/dn denotes an inward normal derivative. In the above equation, if G is chosen to satisfy

$$\nabla_t^2 G(k,\bar{r},\bar{r}') + k^2 G(k,\bar{r},\bar{r}') = -\delta(|\bar{r}-\bar{r}'|) \tag{3}$$

where the delta function is defined in a way such that the value of its volume integral is unity, then (2) reduces to the form of

$$F(\bar{r}) = \oint_C \left[F(\bar{r}')\frac{dG(k,\bar{r},\bar{r}')}{dn} - G(k,\bar{r},\bar{r}')\frac{dF(\bar{r}')}{dn}\right] d\bar{r}'. \tag{4}$$

It can be verified that the function taking the form of $[(1/4j)H_0^{(2)}(k|\bar{r}-\bar{r}'|)]$, known as the two-dimensional Green's function, satisfies (3). Note that k may be a real or pure-imaginary quantity. In the limit of the field point to be calculated approaching the boundary, (4) becomes

$$\frac{1}{2}F(\bar{r}) = \int_C F(\bar{r}')\frac{dG(k,\bar{r},\bar{r}')}{dn}d\bar{r}' - \oint_C G(k,\bar{r},\bar{r}')\frac{dF(\bar{r}')}{dn}d\bar{r}' \tag{5}$$

where $\int$ denotes the Cauchy principal value integral with the singularity at the point of $\bar{r}' = \bar{r}$ being removed. In deriving (5), the boundary in the vicinity of the singularity is approximated by a straight segment and the contribution of the singularity is determined by deforming outward the integration contour at $\bar{r}$ into a semicircle with a vanishing radius and using the property of the Hankel function with vanishing arguments. (For an angled segment, the contribution can be determined in a similar way.) The relation between F and dF/dn for each one of the regions involved is independent of other regions and is solved separately. The relation among all the regions is carried through the continuity requirement of some associated fields, as follows.

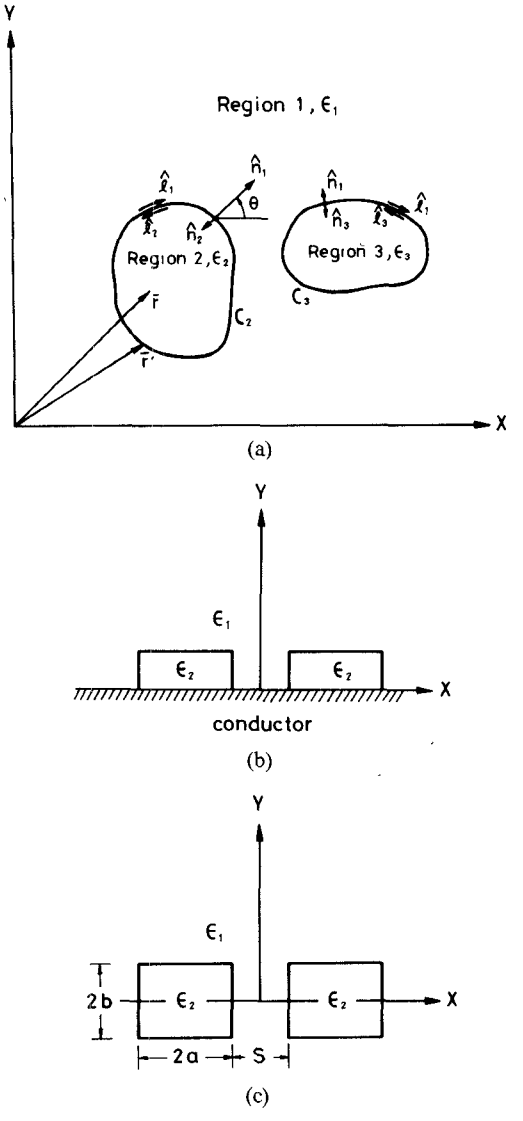

Fig. 1. Cross sections of the guiding structures. (a) Two coupled dielectric waveguides of arbitrary cross sections. (b) Two identical, coupled dielectric image lines of rectangular cross sections. (c) Two identical, coupled dielectric waveguides of rectangular cross sections.

In the rigorous vector form, the four kinds of tangential fields (E_z, H_z, E_l, and H_l) should be made continuous across the boundaries where permittivity discontinuity exists. While not all of these fields are needed in the formulation, since some fields can be related through Maxwell's equations to other fields. One of the ways is to formulate them in terms of the axial component, from which the transverse tangential fields can be obtained as

$$E_l = \frac{-j\beta}{k^2}\left[\frac{\partial E_z}{\partial l} + \frac{\omega\mu_0}{\beta}\frac{\partial H_z}{\partial n}\right] \tag{6a}$$

and

$$H_l = \frac{-j\beta}{k^2}\left[\frac{\partial H_z}{\partial l} - \frac{\omega\epsilon}{\beta}\frac{\partial E_z}{\partial n}\right] \tag{6b}$$

where $\partial/\partial l$ denotes the derivative in the $\hat{l}$ direction as

depicted in Fig. 1(a). However, it is found from the calculation that for some modes, this $E_z - H_z$ formulation yields unreliable results in the near cutoff region. Such trouble is believed due to the presence of the denominator k^2 in (6) for the cladding region, since the numerical errors in the brackets of (6) will be augmented when the corresponding denominator k^2 becomes small. Further, such a denominator vanishes at cutoff and, hence, makes it difficult in treating cutoff frequencies. Another way is to formulate them in terms of transverse fields ($E_x - E_y$ or $H_x - H_y$). It is noted that, due to the fact that the transverse magnetic fields are continuous at a permittivity discontinuity, it is of considerable convenience to employ the $H_x - H_y$ formulation, in which the longitudinal fields (E_z and H_z) can be obtained respectively from the relations of $j\omega\epsilon\bar{E} = \nabla \times \bar{H}$ and $\nabla \cdot \bar{H} = 0$ as

$$j\omega E_z = \left(\frac{\partial H_n}{\partial l} - \frac{\partial H_l}{\partial n} \right) \Big/ \epsilon \tag{7a}$$

and

$$j\beta H_z = \frac{\partial H_n}{\partial n} + \frac{\partial H_l}{\partial l} \tag{7b}$$

where H_n denotes the component in the $\hat{n}$ direction. Explicitly,

$$H_n = H_x \cos\theta + H_y \sin\theta$$
$$H_l = H_x \sin\theta - H_y \cos\theta$$

and θ is the angle from the x direction to $\hat{n}$. Note that from the relation of $-j\omega\mu_0\bar{H} = \nabla \times \bar{E}$, it can be shown that the transverse tangential electric field E_l has been made continuous at the boundaries in the $H_x - H_y$ formulation. Thus, from (7), one obtains a complete description of the whole guiding structure in terms of H_x and H_y and their normal derivatives at all the boundaries encountered. By matching the longitudinal fields at such boundaries and using the relation of (5), the propagation characteristics can be determined. Once the eigenvalues and the associated eigenfunctions are found, the corresponding field patterns can be obtained from (4).

As the differences among the permittivities of all the regions become small enough, any transverse-field component in rectangular coordinates satisfies the Helmholtz equation everywhere and, consequently, such a field and its normal derivative are continuous everywhere in the entire space. Thus, one can formulate the propagation problem in terms of such a field and obtain the propagation characteristics in the scalar form by matching its normal derivative at all the boundaries encountered.

In case the cross section of a guiding structure possesses symmetry about some axis, the field patterns of guided modes will be of either *reflection* or *anti-reflection* about that axis. Therefore, if H_x is symmetric about that axis, H_y will be antisymmetric, and vice versa. Due to the opposite symmetry between H_x and H_y, we refer hereafter to the symmetry type with respect to H_y. Note that the associated fields and their normal derivatives possess the same symmetry. By utilizing such a symmetry property, the orders of the resultant matrices in Section IV can be reduced.

III. Green's Function at Cutoff

At cutoff, $\beta^2 \to k_0^2\epsilon_1$, here ϵ_1 is the relative permittivity of the cladding. Under such a situation, the Green's function for the cladding becomes singular as the argument of the corresponding Hankel function vanishes. In view of this, the Green's function at cutoff is treated otherwise, as follows.

A function that satisfies (3) with $k = 0$ may be constructed from $[A_1 + A_2 \ln|\bar{r} - \bar{r}'|]$. We substitute such a quantity into (3) and integrate both sides of (3) over a domain containing the point of $\bar{r}$. Using the integration to cancel two factors which otherwise lead to singularities, it is found that $A_2 = -1/2\pi$, while A_1 remains undetermined; in other words, A_1 may take any value. From the calculation, it is found that, except for some modes, no substantial deviation of the result is observed while the value of A_1 is varied over several orders of magnitude. As to the exception modes, their cutoff values are found to deviate a few percent when the numerical values of Green's function distribute around zero. In view of this, we choose a value of A_1 such that all the values of Green's function encountered are away from zero (say, greater than 10 or less than -10).

IV. Numerical Procedure

The coupled equations (5) and (7) are solved by point-matching. Around the integration contour C_i, we choose N_i node points at which the unknown fields and their normal derivatives are to be solved. Then the integrations in (5) are discretized into summations. The quantities of Green's functions and their normal derivatives are evaluated between two associated node points, except when such two points coincide, or when they come very close in the multiple-cylinder case. In such situations, some finer evaluation is used. Thereafter, for region i one obtains N_i simultaneous equations with the $2N_i$ unknowns being the values of F and dF/dn at the N_i node points. From these equations, one can express explicitly dF/dn in term of F by solving the corresponding $N_i \times N_i$ matrix, which is complex when $\beta^2 < k_0^2\epsilon_i$ and is real otherwise. Once the explicit relations are solved for every region, they are substituted in (7) for corresponding regions. The differentiation $(\partial H_n/\partial l)$ in (7a) is approximated by a three-point finite-difference for general cases of irregularly-spaced node points. The differentiation $(\partial H_l/\partial l)$ in (7b) is continuous automatically and is deleted in actual calculation. It is noted that since all the transverse fields of guided modes are real quantities, the imaginary parts of those complex explicit relations are deleted. Then, from the continuity requirement, one arrives at a $2N \times 2N$ real matrix ($N = N_1$, the number of node points of region 1 or the sum of N_i's of all the other regions) with the unknowns being H_x and H_y at the N node points. By searching the roots of its determinant, one can determine the propagation characteristics of guided modes in the rigorous vector form. As to the scalar form, after the explicit relations are obtained (the same ones of the vector form), one immediately arrives at an $N \times N$ real matrix by matching the normal derivatives at

the N node points. Note that by utilizing the symmetry property, the orders of all the matrices involved are deduced to one-half or one-fourth for the one-fold or two-fold symmetry, respectively.

V. Result

The following calculation is addressed to single and double (in the latter case, the two coupled waveguides are made to be identical) waveguides of circular and rectangular cross sections, and the results are presented in normalized quantities: normalized propagation constant B, the conventional normalized frequency V of a circular waveguide (with radius a), and another normalized frequency V_s, which is convenient for a rectangular waveguide (with one side length of $2b$), where

$$B = \left[(\beta/k_0)^2 - \epsilon_1\right]/(\epsilon_2 - \epsilon_1)$$

$$V = k_0 a(\epsilon_2 - \epsilon_1)^{1/2}$$

and

$$V_s = 2k_0 b(\epsilon_2 - \epsilon_1)^{1/2}/\pi.$$

By using such normalized quantities, the propagation characteristics are determined by the permittivity ratio $\epsilon_r (= \epsilon_2/\epsilon_1)$, not necessarily by their respective values.

To check the accuracy, this method is first applied to circular waveguides of the step profile. As shown in Fig. 2, the agreement between the calculated results for $N = 20$ and the exact solutions is fairly good for both the vector and scalar forms, especially for the fundamental mode. Only the HE modes are shown in Fig. 2(a); for other modes (TE_{01}, TM_{01}, and EH_{11}), the accuracy is seen to be of about the same degree. We have also checked the results of some lower modes of rectangular waveguides with aspect ratios ($= a/b$ in Fig.1(c)) of 1 and 2 with those by the circular-harmonic expansion [1], and the discrepancy is within the accuracy of reading the drawings. In the following discussion, N is chosen to be 24 or 48 for single or double waveguides, respectively.

In contrast to the method of circular-harmonic expansion, the present method is capable of treating waveguides of rather elongated cross sections in both the vector and scalar forms, as shown respectively in Figs 3 and 4 for a rectangular waveguide with an aspect ratio of 5. For the rectangular waveguides, we follow a similar mode designation of Goell [1], namely, $H^x_{mn}(H^y_{mn})$ denotes a mode of which the dominant transverse magnetic field is directed in the $x(y)$ direction and the dominant field pattern has m and n peaks in the x and y directions, respectively. Note that the $E^x_{mn}(E^y_{mn})$ modes in [1] correspond to the present $H^y_{mn}(H^x_{mn})$ modes. Comparing the dispersion curves in Figs. 3 and 4, one can find a similar phenomenon discussed in [1], that is, the permittivity ratio has a stronger effect on the H^x_{mn} modes than the H^y_{mn} modes. Fig. 5 illustrates the dispersion curves of two coupled dielectric image lines with rectangular cross sections as depicted in Fig. 1(b). Due to the conducting plate, the propagation modes correspond to those modes with H_y (or, correspondingly, E_x) antisymmetric about the x axis when the structure of Fig. 1(c) is used instead. Due to the coupling

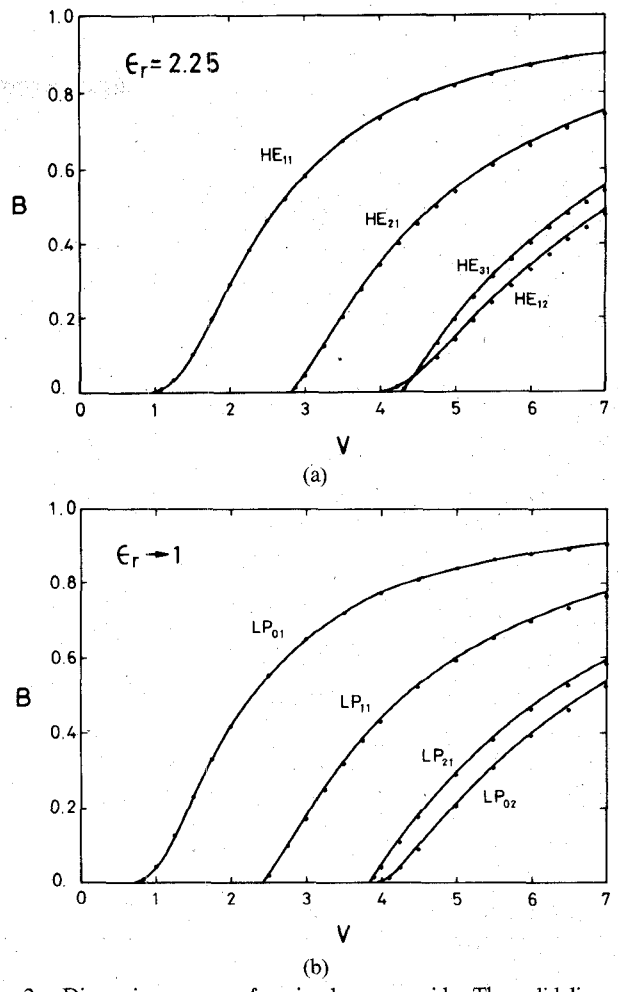

Fig. 2. Dispersion curves of a circular waveguide. The solid lines are exact solutions and the dots (●) represent the calculated results with $N = 20$. (a) Vector form. (b) Scalar form.

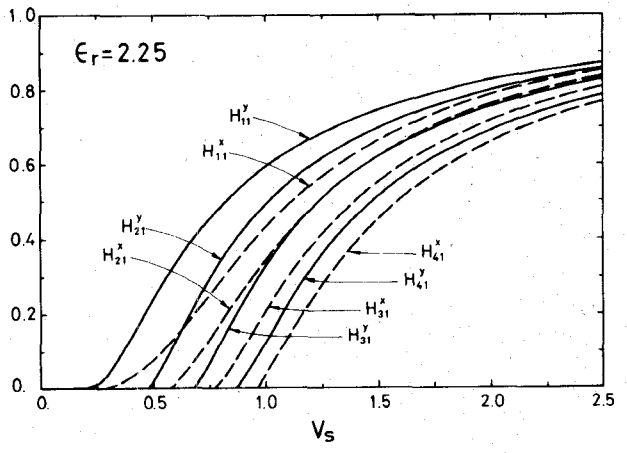

Fig. 3. Vectorial dispersion curves of the first eight modes of a rectangular waveguide with an aspect ratio of 5.

between such two nearby waveguides, each mode of an isolated waveguide is split into two modes: one symmetric and one antisymmetric about the y axis. From Fig. 5, it is seen that the curve of an isolated waveguide sits between the two corresponding split modes. Comparing the results in [10] and Fig. 5, we find a discrepancy of several percent between them, except in the near-cutoff region. We have checked the results with larger values of N, and no sub-

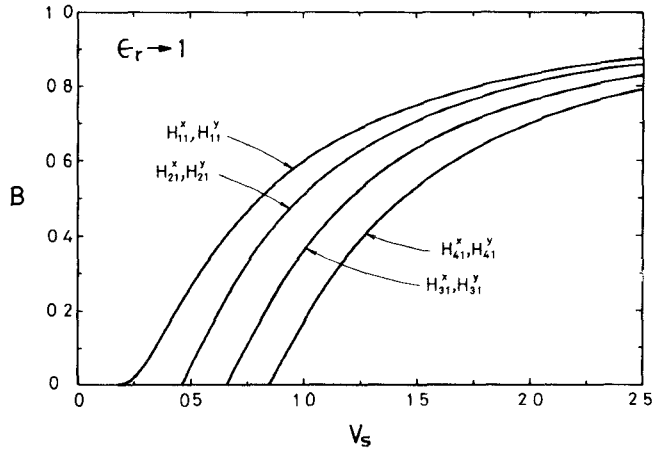

Fig. 4. Scalar dispersion curves of the first four nondegenerate modes of a rectangular waveguide with an aspect ratio of 5.

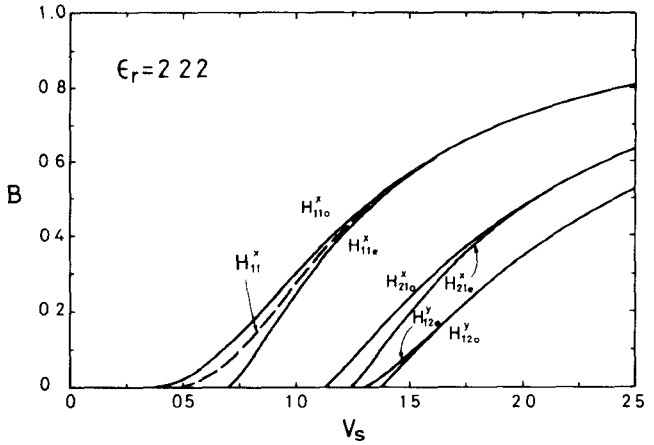

Fig. 5. Vectorial dispersion curves of coupled dielectric image lines of rectangular cross sections with an aspect ratio of 1.39 and a separation s/a of 1.02 (see Fig. 1(c)). An additional subscript $e(o)$ is added to the mode designation for those modes symmetric or even (antisymmetric or odd) about the y axis. The dashed line is the fundamental mode of the corresponding isolated image line.

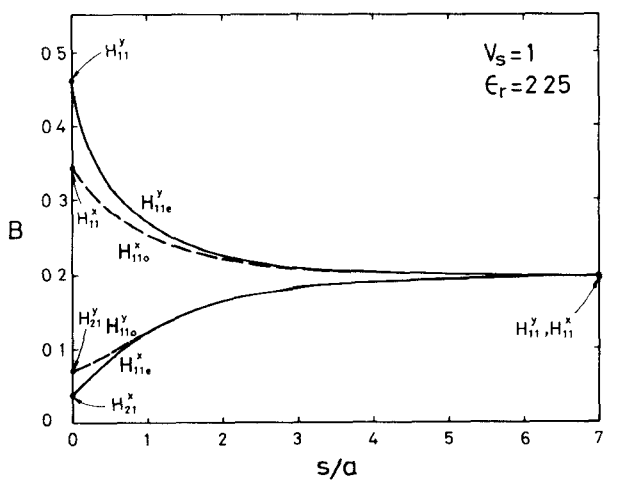

Fig. 6. Splitting of the H_{11}^y and H_{11}^x modes (■) of square waveguides as a function of the separation s. The dots (●) indicate the first four modes of a rectangular waveguide with an aspect ratio of 2.

stantial changes are observed in our results. The magnitude of splitting in coupled waveguides as a function of the separation s is illustrated in Fig. 6 for two coupled waveguides of square cross sections. When these two waveguides are far apart ($s \to \infty$), the guided modes correspond

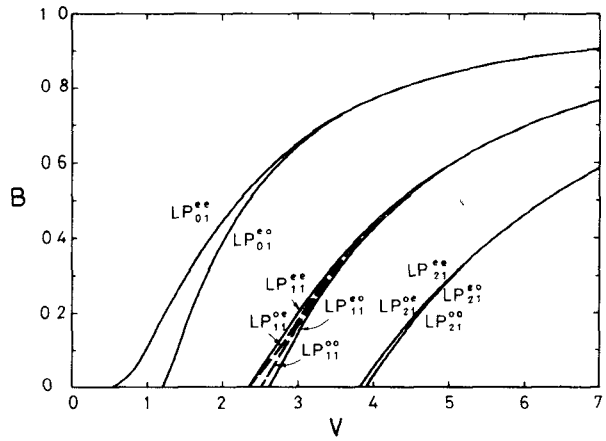

Fig. 7. Scalar dispersion curves of two coupled circular fibers with $s/a = 1$. (Here, s is given by the distance between the two centers minus the diameter $2a$.) The discrepancies between the LP_{21}^{ee} and LP_{21}^{oe} modes and between the LP_{21}^{eo} and LP_{21}^{oo} modes are too small to be shown in the drawing.

to those of a single waveguide; as they come closer, the splitting becomes larger. In the limit of the separation s approaching zero, the split modes become the modes of a single waveguide with a double aspect ratio. Similar splitting due to the mutual coupling also exists in the coupled circular waveguides (with the rectangular cross sections in Fig. 1(c) being replaced by circular ones), as illustrated in Fig. 7 for the scalar form. While each circular LP_{ml} mode (except those modes with the azimuthal mode number $m = 0$) is split into 4 modes: the LP_{ml}^{ee} (symmetric and symmetric about the x and y axis, respectively), LP_{ml}^{eo} (symmetric and antisymmetric), LP_{ml}^{oe} (antisymmetric and symmetric), and LP_{ml}^{oo} (antisymmetric and antisymmetric) modes. As to the modes with $m = 0$, since their field patterns should be symmetric about the x axis, only two split modes exist. From Figs. 5 and 7, it is found that the splitting is stronger for a lower value of B or for lower modes, especially for the fundamental modes. It indicates that for given propagation constants the fields of the fundamental modes penetrate farthest into the outer cladding.

Using Green's function at cutoff for the cladding (region 1 in Fig. 1), cutoff frequencies of the guided modes can be determined. Calculated normalized cutoff frequencies of the circular LP_{11}, LP_{21}, and LP_{02} modes are 2.408, 3.849, and 3.867, respectively; the corresponding exact solutions are 2.405, 3.832, and 3.832, respectively. Results of isolated and coupled rectangular waveguides are presented in Table I. For comparison, we also list the corresponding normalized frequencies at a very small value of B, (say, $B = 0.0001$). From the results, it is found that, for some modes, the frequencies at a very small B agree substantially with the corresponding cutoff frequencies (at $B = 0$); however, for the fundamental modes and some other modes (the exception modes in Section III), the cutoff frequencies are appreciably a little lower. From Table I, it is seen that for an isolated waveguide, there are two fundamental modes that are never cutoff: the H_{11}^y and H_{11}^x modes. As to the coupled waveguides, they still possess two fundamental modes (H_{11e}^y and H_{11o}^x), since the cutoff frequencies of two of the split modes shift from zero.

TABLE I
NORMALIZED CUTOFF FREQUENCIES OF RECTANGULAR WAVEGUIDES WITH $a/b = 2$

Mode	$\epsilon_r \to 1$	$\epsilon_r = 2.25$	Coupled Waveguides $\epsilon_r = 2.25$, $s/a = 2$ even	Coupled Waveguides $\epsilon_r = 2.25$, $s/a = 2$ odd
H^y_{11}	0.00 (0.244)*	0.00 (0.288)	0.00 (0.215)	0.475 (0.476)
H^x_{11}	0.00 (0.244)	0.00 (0.329)	0.537 (0.538)	0.00 (0.253)
H^y_{21}	0.818 (0.819)	0.861 (0.861)	0.840 (0.844)	0.897 (0.898)
H^x_{21}	0.818 (0.819)	0.928 (0.928)	0.959 (0.960)	0.910 (0.913)
H^y_{31}	1.244 (1.261)	1.256 (1.284)	1.254 (1.270)	1.332 (1.332)
H^x_{31}	1.244 (1.261)	1.320 (1.337)	1.367 (1.368)	1.318 (1.328)
H^y_{12}	1.199 (1.200)	1.230 (1.230)	1.216 (1.217)	1.243 (1.244)
H^x_{12}	1.199 (1.200)	1.325 (1.326)	1.347 (1.348)	1.302 (1.304)

*The parenthesized data present the corresponding normalized frequencies at $B = 0.0001$.

VI. CONCLUSION

In this investigation, a method of surface integral equations has been originally developed in the rigorous vector and the scalar forms, which can treat single as well as multiple waveguides of arbitrary cross sections. Green's function at cutoff is also presented to treat the corresponding cutoff frequencies.

Note that the present method cannot be applied directly to those waveguides, such as the slab-coupled waveguides [11], in which the boundary of permittivity discontinuity and, hence, the integration contour extend to infinity. An extension of the present rigorous method to treat such structures is discussed in [12].

Another important extension of the present method is to combine with the finite-element method for treating the more general guiding structures which include some bounded inhomogeneous regions. For such inhomogeneous regions, the explicit relations can be handled by the finite-element method (instead of (5)). Except for this, the other works toward obtaining the propagation characteristics are the same as in this investigation. By using such a combined method, the manipulation of the more time-consuming finite-element method is carried out within only the inhomogeneous regions. It results in a large reduction in computation effort as compared with other methods in the literature (for a typical example, see [13]), in which the calculation of the finite-element method has to be extended far into the outer homogeneous regions.

REFERENCES

[1] J. E. Goell, "A circular-harmonic computer analysis of rectangular dielectric waveguides," *Bell Syst. Tech. J.*, vol. 48, pp. 2133–2160, Sept. 1969.

[2] A. L. Cullen, O. Özkan, and L. A. Jackson, "Point-matching technique for rectangular-cross-section dielectric rod," *Electron. Lett.*, vol. 7, pp. 497–499, Aug. 1971.

[3] C. C. Su, "Cutoff frequency of a homogeneous optical fiber with arbitrary cross-section," *IEEE Trans. Microwave Theory Tech.*, this issue, pp. 1101–1105.

[4] L. Eyges, P. Gianino, and P. Wintersteiner, "Modes of dielectric waveguides of arbitrary cross sectional shape," *J. Opt. Soc. Am.*, vol. 69, pp. 1226–1235, Sept. 1979.

[5] N. Morita, "A method extending the boundary condition for analyzing guided modes of dielectric waveguides of arbitrary cross-sectional shape," *IEEE Trans. Microwave Theory Tech.*, vol. MTT-30, pp. 6–12, Jan. 1982.

[6] H. Shinonaga and S. Kurazono, "Y dielectric waveguide for millimeter- and submillimeter-wave," *IEEE Trans. Microwave Theory Tech.*, vol. MTT-29, pp. 542–546, June 1981.

[7] E. F. Kuester, "Propagation constants for linearly polarized modes of arbitrarily shaped optical fibers or dielectric waveguides," *Opt. Lett.*, vol. 8, pp. 192–194, Mar. 1983.

[8] S. Akiba and A. Haus, "Variational analysis of optical waveguides with rectangular cross section," *Appl. Opt.*, vol. 21, pp. 804–808, Mar. 1982.

[9] E. A. J. Marcatili, "Dielectric rectangular waveguide and directional coupler for integrated optics," *Bell Syst. Tech. J.*, vol. 48, pp. 2071–2102, Sept. 1969.

[10] K. Solbach and I. Wolff, "The electromagnetic fields and the phase constants of dielectric image lines," *IEEE Trans. Microwave Theory Tech.*, vol. MTT-26, pp. 266–274, Apr. 1978.

[11] E. A. J. Marcatili, "Slab-coupled waveguides," *Bell Syst. Tech. J.*, vol. 53, pp. 645–674, Apr. 1974.

[12] C. C. Su, "Analysis of versatile dielectric waveguides using the surface integral equations method," submitted for publication.

[13] N. Mabaya, P. E. Lagasse, and P. Vandenbulcke, "Finite element analysis of optical waveguides," *IEEE Trans. Microwave Theory Tech.*, vol. MTT-29, pp. 600–605, 1981.

✠

Ching-Chuan Su was born in Taiwan on October 2, 1955. He received the B.S., M.S., and Ph.D. degrees in electrical engineering from National Taiwan University in 1978, 1980, and 1985, respectively.

From 1980 to 1982, he was employed in an IC company, where he was responsible for the development of several MOS fabrication processes.

In 1985, he joined the faculty of National Tsing Hua University, Hsinchu, Taiwan, where he currently serves as an Associate Professor in electrical engineering. His theoretical interests include bistability in nonlinear optics and numerical methods in dielectric waveguide body scattering, and MOS device simulation.